Evgeny V. Nazarchuk, Oleg I. Siidra*, Dmitry O. Charkin, Stepan N. Kalmykov and Elena L. Kotova

Effect of solution acidity on the crystallization of polychromates in uranyl-bearing systems: synthesis and crystal structures of $Rb_2[(UO_2)(Cr_2O_7)(NO_3)_2]$ and two new polymorphs of $Rb_2Cr_3O_{10}$

https://doi.org/10.1515/zkri-2020-0078
Received September 3, 2020; accepted January 15, 2021; published online January 26, 2021

Abstract: Three new rubidium polychromates, $Rb_2[(UO_2)(Cr_2O_7)(NO_3)_2]$ (**1**), γ-$Rb_2Cr_3O_{10}$ (**2**) and δ-$Rb_2Cr_3O_{10}$ (**3**) were prepared by combination of hydrothermal treatment at 220 °C and evaporation of aqueous solutions under ambient conditions. Compound **1** is monoclinic, $P2_1/c$, a = 13.6542(19), b = 19.698(3), c = 11.6984(17) Å, β = 114.326(2)°, V = 2867.0(7) Å^3, R_1 = 0.040; **2** is hexagonal, $P6_3/m$, a = 11.991(2), c = 12.828(3) Å, γ = 120°, V = 1597.3(5) Å^3, R_1 = 0.031; **3** is monoclinic, $P2_1/n$, a = 7.446(3), b = 18.194(6), c = 7.848(3) Å, β = 99.953(9)°, V = 1047.3(7) Å^3, R_1 = 0.037. In the crystal structure of **1**, UO_8 bipyramids and NO_3 groups share edges to form $[(UO_2)(NO_3)_2]$ species which share common corners with dichromate Cr_2O_7 groups producing novel type of uranyl dichromate chains $[(UO_2)(Cr_2O_7)(NO_3)_2]^{2-}$. In the structures of new $Rb_2Cr_3O_{10}$ polymorphs, CrO_4 tetrahedra share vertices to form $Cr_3O_{10}^{2-}$ species. The trichromate groups are aligned along the 6_3 screw axis forming channels running in the *ab* plane in the structure of **2**. The Rb cations reside between the channels and in their centers completing the structure. The trichromate anions are linked by the Rb^+ cations into a 3D framework in the structure of **3**. Effect of solution acidity on the crystallization of polychromates in uranyl-bearing systems is discussed.

***Corresponding author: Oleg I. Siidra**, Department of Crystallography, St. Petersburg State University, University Emb. 7/9, 199034 St. Petersburg, Russia; and Kola Science Center, Russian Academy of Sciences, Apatity, 184200 Murmansk Region, Russia, E-mail: o.siidra@spbu.ru
Evgeny V. Nazarchuk, Department of Crystallography, St. Petersburg State University, University Emb. 7/9, 199034 St. Petersburg, Russia
Dmitry O. Charkin and Stepan N. Kalmykov, Department of Chemistry, Moscow State University, Leninskie Gory 1, 119991 Moscow, Russia
Elena L. Kotova, St. Petersburg Mining University, 21st Line, St. Petersburg 199106, Russia

Keywords: hexavalent chromium; polychromates; rubidium; uranium.

1 Introduction

The studies of uranium compounds are of importance from mineralogical [1], material, and environmental [2] aspects. For instance, the composition of nuclear wastes is particularly complex including both “intrinsic” compounds and those formed due to the interaction with materials of containers [3–5]. In the recent decades, essential progress has been achieved in the crystal chemistry of uranium compounds containing tetrahedral anions like sulfate [6–9], selenate [10–12], molybdate [13–20], and tungstate [21–23]. To date, chromate-bearing systems received less attention. However, a series of new uranyl chromate compounds have been prepared and described recently by our group [24–32]. These compounds exemplify the relevance, as potassium chromate and dichromate have been used earlier in the nuclear industry [33]. According to the data obtained by the Khlopin Radium Institute, the chromium content in nuclear wastes can be as high as 0.63 wt. %.

The spent nuclear fuel also contains noticeable amounts of alkali isotopes (Na, K, Rb, Cs) [34, 35], the most abundant being ^{137}Cs (0.3–0.4 wt.%) [36]. The abundance of ^{22}Na, ^{86}Rb, ^{51}Cr isotopes is also significant [4, 37].

The history of alkali uranium compounds dates back to the pioneering works of Kovba et al. (1958) who reported first uranates of K, Rb, and Cs [38]. The first potassium uranyl fluoride, $K_3(UO_2)F_5$ was described in 1954 [39]. The first structural characterization of carnotite, $K(UO_2)(VO_4)$, was performed using a synthetic anhydrous sample [40].

The first potassium uranyl chromate, $K(UO_2)(OH)(CrO_4)(H_2O)_{1.5}$, was reported three decades ago [41]. In 2002, Sykora et al. [42] described a complex rubidium uranyl chromate iodate, $Rb_2(UO_2)(CrO_4)(IO_3)_2](H_2O)$. In 2010, Verevkin et al. [43] reported a first rubidium uranyl chromate

without any other anions, $Rb_2[(UO_2)_2(CrO_4)_3H_2O)](H_2O)_4$. Later on, our group succeeded in preparation of three novel rubidium uranyl chromates, $Rb_2[(UO_2)(CrO_4)_2]$ [31], $Rb_2[(UO_2)(CrO_4)(Cr_2O_7)]$ [44], and $Rb_2[(UO_2)(CrO_4)(NO_3)]$ [30]. The Rb-bearing systems are of particular interest as they home unique uranyl chromates with 3D framework architectures: $Rb_2[(UO_2)_2(CrO_4)_3(H_2O)_2](H_2O)_3$ and $Rb_2[(UO_2)_2(CrO_4)_3(H_2O)](H_2O)$ [45].

Uranyl nitrate hexahydrate is the most common uranium source in solution syntheses of U^{VI} compounds, including chromates. Therefore, the crystallization milieu contains essential amounts of nitrate anions. The latter are similar in size to carboxylates and coordinate in a κ^2-fashion to the equatorial sites of the $(UO_2)O_n$ polyhedra [46]. In this way, they act as terminating ligands reducing the dimensionality of the complexes formed [44]. As yet, the architectures containing simultaneously both tetrahedral and trigonal oxyanions are very rare (Table 1), and most of them are found among uranyl chromates. The 0*D* $[(UO_2)(Cr_2O_7)(NO_3)_2]_2^{4-}$ unit (Figure 1a) was observed in the structure of $Cs_2[(UO_2)(Cr_2O_7)(NO_3)_2]$ [44]. It is formed by two UO_8 hexagonal bipyramids, four terminal κ^2-NO_3^- triangles, and two bridging $Cr_2O_7^{2-}$ dichromate groups. These compounds were obtained in a two-step synthesis including hydrothermal treatment and subsequent room-temperature evaporation. The initial "hydrothermal" step is conducted at 90 °C. The same approach also resulted in formation of $[i\mathrm{PrNH_3}][(UO_2)(CrO_4)(NO_3)]$ [26], wherein the framework is comprised of $[(UO_2)(CrO_4)(NO_3)]^-$ chains (Figure 1b) linked by isopropylammonium cations via hydrogen bonds. Note that both syntheses ($Cs_2[(UO_2)(Cr_2O_7)(NO_3)_2]$ and $[i\mathrm{PrNH_2}][(UO_2)(CrO_4)(NO_3)]$) started from the same ratio of $UO_2(NO_3)_2{\cdot}6(H_2O)$:$CrO_3$ = 1:20.

The $[(UO_2)(TO_4)(NO_3)]^-$ chains (Figure 1b) are found in the structures of uranyl chromates [50] and sulfates [47]; a very similar topology is observed also for selenites [48]. Attachment of nitrate groups to the uranyl cations results in unique topologies. The $[(UO_2)_2(CrO_4)_2(NO_3)_2(H_2O)]^{2-}$ chains, observed in the structure of $(Me_2NH_2)_2[(UO_2)_2(NO_3)_2(CrO_4)_2(H_2O)]H_2O$ [49] are constructed from terminal $[UO_2(NO_3)_2]$ species attached to $[UO_2(CrO_4)_2]^{2-}$ chains; note two different coordination modes of uranium (UO_7 and UO_8 bipyramids, Figure 1c).

The structure of $A[(UO_2)(CrO_4)(NO_3)]$ (A = K, Rb) [30] contains unique and rather complex corrugated layers, shown in Figure 1d, wherein the nitrate groups also serve as terminating ligands. These compounds were prepared via a solid-state route. The CrO_3:$UO_2(NO_3)_2$:ACl ratio was 20:1:2. The mixture was slowly heated to 270 °C, cooled down to 100 °C at 3 °C/h, and to room temperature, at 7 °C/h.

Table 1: Uranium compounds containing mixed-anion complexes with nitrate and sulfate, chromate, or selenite anions.

No.	Formula and external cation species	Figure	Sp. gr.	*a*, Å/α,°	*b*, Å/β,°	*c*, Å/γ,°	*V*, Å^3	Ref.
1	$Cs_2[(UO_2)(Cr_2O_7)(NO_3)_2]$ Cesium	Figure 1a	*P*-1	8.148(3)/70.881(8)	8.299(3)/88.966(9)	11.805(4)/101.782(15)	740.5(4)	[44]
2	$(i\mathrm{PrNH_3})[(UO_2)(CrO_4)(NO_3)]$ Isopropylammonium	Figure 1b	*P*-1	7.245(3)/85.549(6)	7.329(3)/82.547(6)	11.359(4)/80.174(6)	588.3(4)	[26]
3	$(NMe_4)(UO_2(SO_4)(NO_3))$ Tetramethylammonium	Figure 1b	*C*2/*m*	21.1060(10)	6.9350(3)/97.5468(18)	8.4284(5)	1222.98(2)	[47]
4	$(NMe_4)(UO_2(NO_3)(Se^{VI}O_3))$ Tetramethylammonium	Figure 1b	*C*2/*m*	21.888(3)	6.9501(8)/97.618(3)	8.3495(10)	1258.94(3)	[48]
5	$(Me_2NH_2)_2[(UO_2)_2(NO_3)_2(CrO_4)_2(H_2O)]H_2O$ Dimethylammonium	Figure 1c	*P*-1	8.384(5)/73.444(10)	10.715(6)/85.231(10)	14.211(8)/71.646(10)	1161.4(11)	[49]
6	$K[(UO_2)(CrO_4)(NO_3)]$ Potassium	Figure 1d	$P2_1/c$	9.881(5)	7.215(4)/124.85(3)	14.226(6)	832.3(7)	[30]
7	$Rb[(UO_2)(CrO_4)(NO_3)]$ Rubidium	Figure 1d	$P2_1/c$	9.804(1)	7.359(1)/122.048(4)	14.269(1)	872.6(1)	[30]

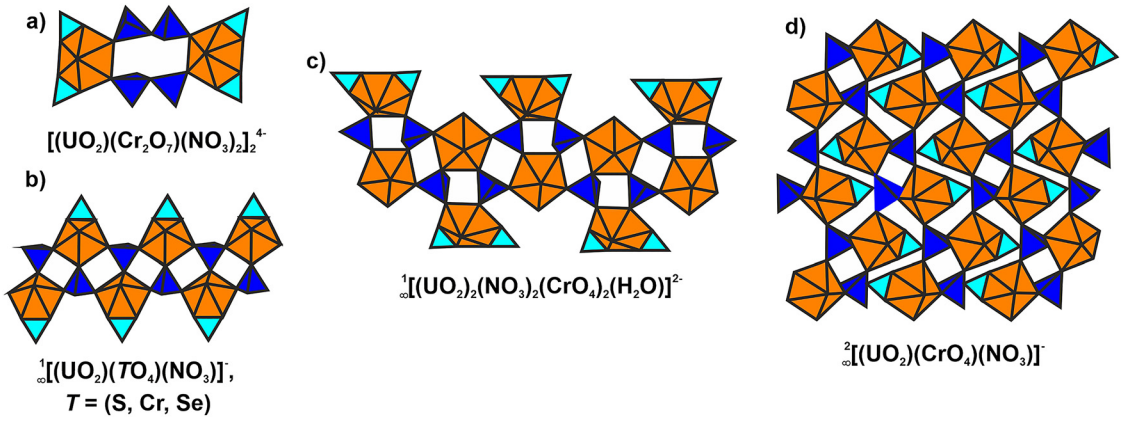

Figure 1: Uranyl-based architectures containing NO_3^- and $T^{VI}O_4^{2-}$ (T = S, Cr) or $Se^{IV}O_3^{2-}$ anions. The isolated complex in the structure of $Cs_2[(UO_2)(Cr_2O_7)(NO_3)_2]$ (a). Chains found in the structures of $[i\text{PrNH}_3][(UO_2)(CrO_4)(NO_3)]$ (b) and $(Me_2NH_2)_2[(UO_2)_2(NO_3)_2(CrO_4)_2(H_2O)]H_2O$ (c). Unique layers described in the structures of $A[(UO_2)(CrO_4)(NO_3)]$ (A = K, Rb) (d). The uranium polyhedra are yellow and chromium is dark blue. The nitrate anions are sky blue.

Therefore, all syntheses which have led to formation of mixed-anion uranyl chromates started from the same U^{VI}:Cr^{VI} ratio and included treatment at elevated temperatures. Indeed, cases are known when the nitrate ion is present in the structure as an isolated species not incorporated into the uranyl-based species, *e.g.*, in $K_8[(UO_2)(CrO_4)_4](NO_3)_2$ and $K_5[(UO_2)(CrO_4)_3](NO_3)\ (H_2O)_3$ [51]. In these cases, the source of Cr^{VI} was not CrO_3 but K_2CrO_4 and thermal treatment was not performed. The compositions of the uranyl chromate species demonstrate essentially higher CrO_4^{2-}:UO_2^{2+} ratio. Given high concentration of chromate dianions, their coordination to the uranyl cation is more electrostatically favorable compared to the nitrate monoanion. It looks likely that the main factor affecting formation of uranyl chromate complexes is the pH- and concentration-sensitive equilibria between the various Cr^{VI}-containing species in solution which associate with uranyl cations upon crystallization.

What differs the CrO_4^{2-} tetrahedra from other anions (S, Se, Mo) is its ability to polymerize in aqueous solutions under rather mild conditions which results in formation of isopolychromate chains such as $Cr_2O_7^{2-}$ [52], $Cr_3O_{10}^{2-}$ [53], or even $Cr_4O_{13}^{2-}$ [54] which incorporate into the structures of the uranyl compounds [44]. This yields structures containing monochromate [55], dichromate [52] and trichromate [56] anions, as well as mixed-anion species [24]. The SO_4^{2-} and SeO_4^{2-} do not polymerize in aqueous solutions while MoO_4^{2-} and WO_4^{2-} convert into polyoctahedral ensembles upon even mild acidification.

Only six alkali and ammonium trichromates are known to date (Table 2). Note that Li or Na compounds have not been reported. To date, relationships between the size of the alkali cation and the observed set of polymorphic forms were not addressed. These compounds adopt four space groups: *Pbca* for the α-phase, *R3c* for the β-phase, $P6_3/m$ for the γ-phase, and $P2_1/n$ for the δ-phase. Note that our experiments with cesium and potassium species aimed at

Table 2: Crystal data for known alkali/ammonium trichromates.

No.	Compound	Sp. gr.	*a*, Å/α,°	*b*, Å/β,°	*c*, Å/γ,°	*V*, Å^3	*Z*	Ref.
1	α-$(NH_4)_2Cr_3O_{10}$	*Pbca*	11.2558(3)	9.3193(3)	18.9819(5)	1991.13(10)	8	[53]
2	α-$Rb_2Cr_3O_{10}$	*Pbca*	11.521(2)	9.364(2)	19.037(3)	2053.76(65)	8	[58]
3	α-$Cs_2Cr_3O_{10}$	*Pbca*	11.887(2)	9.671(2)	19.493(4)	2240.90(75)	8	[57]
4	β-$Cs_2Cr_3O_{10}$	*R3c*	12.350(2)		38.731(12)	5115.91(229)	18	[59]
5	γ-$(NH_4)_2Cr_3O_{10}$	$P6_3/m$	11.945(3)		12.797(5)	1581.29(101)	6	[60]
6	γ-$Rb_2Cr_3O_{10}$	$P6_3/m$	11.991(2)		12.828(3)	1597.3(5)	6	This work
7	δ-$K_2Cr_3O_{10}$	$P2_1/n$	7.618(3)	17.791(8)/99.20(5)	7.354(3)	983.88(73)	4	[61]
8	δ-$Rb_2Cr_3O_{10}$	$P2_1/n$	7.446(3)	18.194(6)/99.953(9)	7.848(3)	1047.3(7)	4	This work

various uranyl chromates and conducted at pH ≤ 2, had commonly produced bright red crystals of α-$Cs_2Cr_3O_{10}$ and more rarely of δ-$K_2Cr_3O_{10}$.

In this paper, we report the syntheses and structures of three new rubidium polychromates. Formation of the target compound $Rb_2[(UO_2)(Cr_2O_7)(NO_3)_2]$ was accompanied by two uranium-free by-products which occurred to be the "missing" γ- and δ-forms of $Rb_2Cr_3O_{10}$.

2 Experimental section

2.1 Synthesis

Caution! While the compounds of depleted uranium are only weakly radioactive, their chemical toxicity, as well as those of the chromium(VI), is very high. All safety precautions should be followed strictly.

Crystals of **1–3** were synthesized from a solution of 0.05 g of $(UO_2)(NO_3)_2{\cdot}6H_2O$ (Vekton, 99.7%), 0.1 g of CrO_3 (Vekton, 99.7%), 0.4 g of RbCl (Vekton, 99.7%) and 2–10 ml of ultrapure water. The solution was placed in a Teflon-lined Parr reaction vessel and heated to 220 °C for 72 h (3 °C/h), followed by slow cooling to ambient temperature. The cooling rate was 1 °C/h. In all cases, homogeneous solution was obtained which were left to slowly evaporate in fume hoods at ambient conditions. The crystals of **1** formed within 10–15 days as aggregates of red transparent plates up to 0.2 mm in maximum dimension; they precipitated from the acidic solution (pH = 2.5) initially containing 10 ml of water. A Mettler-Toledo Fiveeasy Plus pH FEP20 pH meter was used. These crystals were taken out of the solution which was left for further evaporation. The crystals of **2** and **3** were consecutively formed in two days. After crystallization of **2**, the pH was 2; after crystallization of **3**, 1.5. The crystals of **2** and **3** can coexist in contact with the mother liquor. The former are bright red hexagonal platelets while the latter form spherolites. All crystals were formed at the edges of the solution drops which slowly converted into an amorphous dark brown gel-like substance probably containing some uranium and chromium species.

2.2 X-ray experiment

Selected single crystals were attached to glass fibers using an epoxy resin and mounted on a Bruker SMART APEX II DUO diffractometer equipped with a micro-focus X-ray tube utilizing Mo*K* radiation. The experimental data sets were collected at 100 K. More than a hemisphere of X-ray diffraction data with frame widths of 0.3° in ω, and with 30 s spent counting for each frame were collected. The data were integrated and corrected for absorption using an empirical ellipsoidal model using the Bruker programs APEX and XPREP. Unit cell parameters were calculated using least-squares fits. Structure factors were derived using APEX 2 after introducing the required corrections. Crystal structures were solved using direct methods. The SHELX program package was used for all structural calculations [62]. Further details are collected in Table 3. The final models include site coordinates and anisotropic thermal parameters for all atoms.

3 Results

The structure of **1** contains two symmetrically independent uranium atoms (Figure 2a, b) each forming the uranyl

Table 3: Crystallographic data and refinement parameters for $Rb_2[(UO_2)(Cr_2O_7)(NO_3)_2]$ (**1**), γ-$Rb_2Cr_3O_{10}$ (**2**), and δ-$Rb_2Cr_3O_{10}$ (**3**).

	1	2	3
Space group	$P2_1/c$	$P6_3/m$	$P2_1/n$
a(Å)	13.6542(19)	11.991(2)	7.446(3)
b(Å)	19.698(3)	11.991(2)	18.194(6)
c(Å)	11.6984(17)	12.828(3)	7.848(3)
β, °	114.326(2)		99.953(9)
V(Å^3)	2867.0(7)	1597.3(5)	1047.3(7)
Z	2	6	4
D_x (g/cm^3)	3.619	3.037	3.089
Crystal size, mm	0.12 × 0.16 × 0.10	0.04 × 0.14 × 0.07	0.05 × 0.09 × 0.22
θ max, °	27.99	36.03	27.99
h, k, l range	$-18 \le h \le 18$,	$-19 \le h \le 19$	$-1 \le h \le 9$
	$-26 \le k \le 26$	$-19 \le k \le 19$	$-17 \le k \le 20$
	$-14 \le l \le 15$	$-21 \le l \le 20$	$-10 \le l \le 9$
Measured/independent reflections	6919/5423	2580/1800	1488/1229
R_{int}	0.047	0.057	0.012
R_{sigma}	0.038	0.031	0.030
wR_1	0.102	0.054	0.092
R_1	0.040	0.031	0.037
S	1.033	1.079	1.050
ρmax, min/e Å^{-3}	3.902/−2.474	1.209/−0.818	0.863/−0.689
CCDC	2026269	2026270	2026271

Experiments were carried out at 100 K with MoKα radiation on Bruker Smart DUO, CCD.

cation (<U–O> = 1.767, 1.769 Å, for U1 and U2, respectively). The uranyl cations are almost linear. The O9–U1–O3 and O6–U2–O14 angles are 176.88 and 175.15 respectively. The latter (further denoted as *Ur*) are each coordinated by six oxygen atoms in the equatorial plane (<*Ur*–O> = 2.461, 2.456 Å, respectively). Four symmetrically unique chromium atoms (Figure 2c, d) form $(CrO_4)^{2-}$ tetrahedra (<Cr–O> = 1.649, 1.567, 1.642, and 1.644 Å, respectively).

The Rb1–Rb3 atoms (Figure 2e–g) are coordinated by 10 oxygen atoms each (d(Rb–O) ≤ 3.5 Å; <d(Rb–O)> = 3.131, 3.134, and 3.175 Å, respectively), and Rb4 – by 8 (<d(Rb4–O)> = 3.086 Å) (Figure 2h).

In the structure of **1,** the $Cr1O_4$ and $Cr3O_4$ share a common O8 vertex (Figure 2c), while $Cr2O_4$ and $Cr4O_4$, an O24 vertex (Figure 2d). The Cr–O_{br} distances are relatively long (1.781, 1.772, 1.792, and 1.759 Å), which is in a good agreement with previously published data [61, 63]. Two NO_3^- groups occupy two edges in the equatorial plane of the UO_8 bipyramid to form a terminal $(UO_2)(NO_3)_2$ species. These groups associate with the dichromate anions to form $[(UO_2)(Cr_2O_7)(NO_3)_2]^{2-}$ chains (Figure 3).

The structure of $Rb_2[(UO_2)(Cr_2O_7)(NO_3)_2]$ (Figure 4a, b) corresponds to a new structure type containing chains of a previously unknown architecture. The Rb^+ cations reside between the chains completing the framework.

In the structure of **2**, the Rb1, residing in a special position, centers a trigonal antiprism (<d(Rb1–O)> = 2.960 Å) (Figure 5a), while Rb2 and Rb3 are 10 and 12-coordinated (<d(Rb2–O)> = 3.065, <d(Rb3–O)> = 3.153 Å) (Figure 5b, c). In **3,** the Rb1 and Rb2 (Figure 5e, f) are 11 and 9-coordinated (<d(Rb–O)> = 3.144 and 3.259 Å, respectively). Two symmetrically unique chromium atoms in **2** and three in **3** center the CrO_4 tetrahedra (Figure 5d, g). In both structures these tetrahedra share vertices to form the $Cr_3O_{10}^{2-}$ species.

The trichromate groups are aligned along the 6_3 screw axis forming channels running in the ***ab*** plane (Figure 6a) in the structure of **2**. The Rb cations reside between the channels and in their centers completing the structure. As in the previous case, the trichromate anions are linked by the Rb^+ cations into a 3D framework in the structure of **3** (Figure 6b).

The chromate groups are rather slightly distorted. In **1**, the O–Cr–O angles vary within the 105.4–111.8° range with the mean of 109.45°. In **2** and **3**, these ranges are 106.5–112.2° and 107.62–112.21°, respectively, with the mean of 109.44°. The nitrate groups are close to planar, with deviation angles below 1.29°.

4 Discussion

The structures involving uranyl cations and "pyro" T_2O_7 anions are relatively rare. Among $T^{VI}{}_2O_7^{2-}$ there exists a unique case of (dimorphic) $UO_2(S_2O_7)$ pyrosulfate [64] which does not contain any extra cations. Uranyl-based structural architectures with $T^{V}{}_2O_7^{4-}$ anions were reported among arsenates [65, 66] and phosphates [67]. The degree of polymerization of the chromate tetrahedra increases with increasing Cr^{VI} concentration and decreases with increasing pH [44].

Figure 7 lists the anionic uranyl-dichromate complexes and their graphs. All three species were produced in relatively concentrated solutions at pH 2–2.5. If we consider only

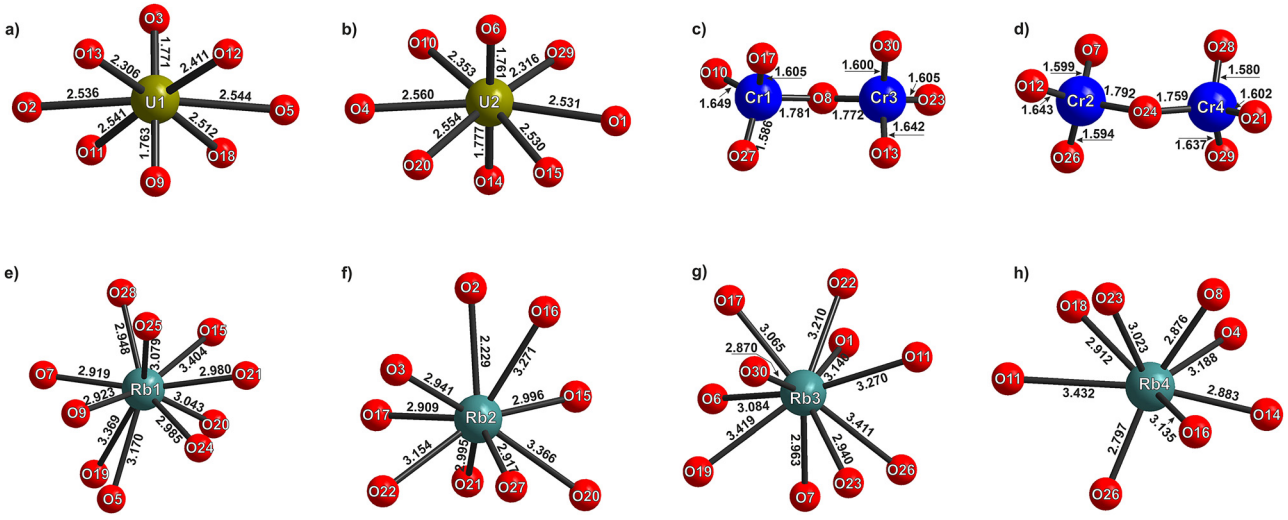

Figure 2: Coordination of U1 (a), U2 (b), Cr1 and Cr3 (c), Cr2 and Cr4 (d), Rb1 (e), Rb2 (f), Rb3 (g), Rb4 (h) in the structure of $Rb_2[(UO_2)(Cr_2O_7)(NO_3)_2]$.

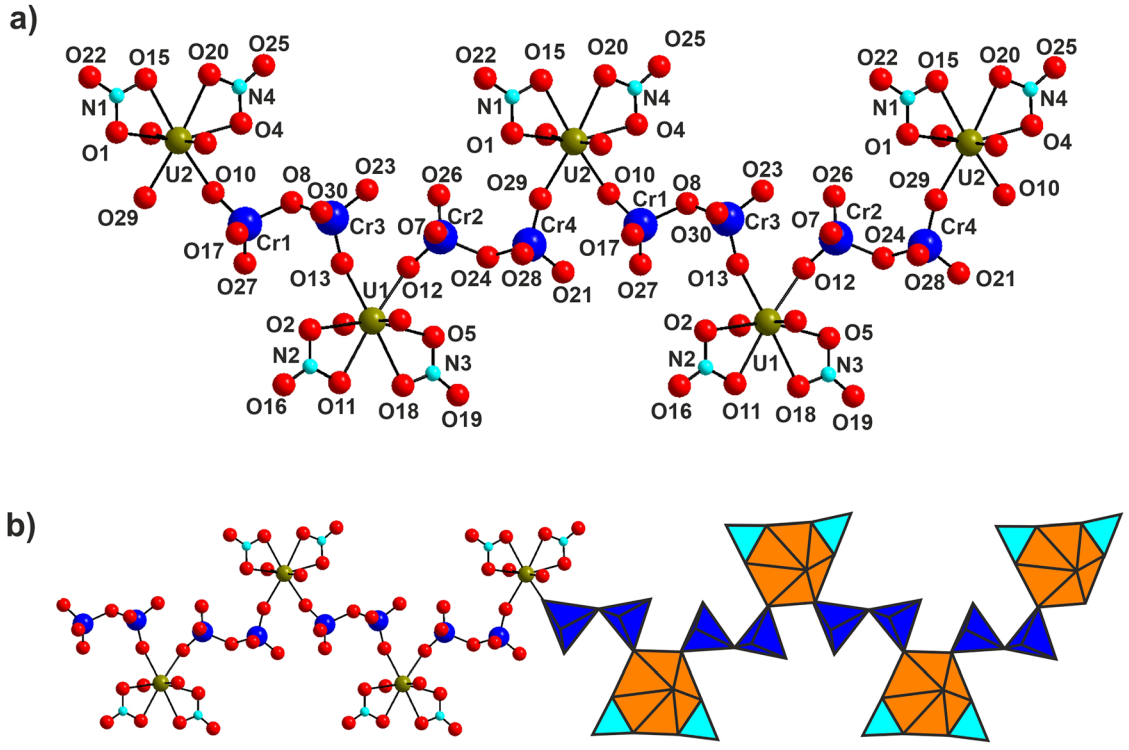

Figure 3: The $[(UO_2)(Cr_2O_7)(NO_3)_2]^{2-}$ chains in the structure of $Rb_2[(UO_2)(Cr_2O_7)(NO_3)_2]$ in ball-and-stick (a) and polyhedral (b) graph representation. The UO_8 polyhedra are shown in yellow, CrO_4 in deep blue, the nitrate groups are sky blue.

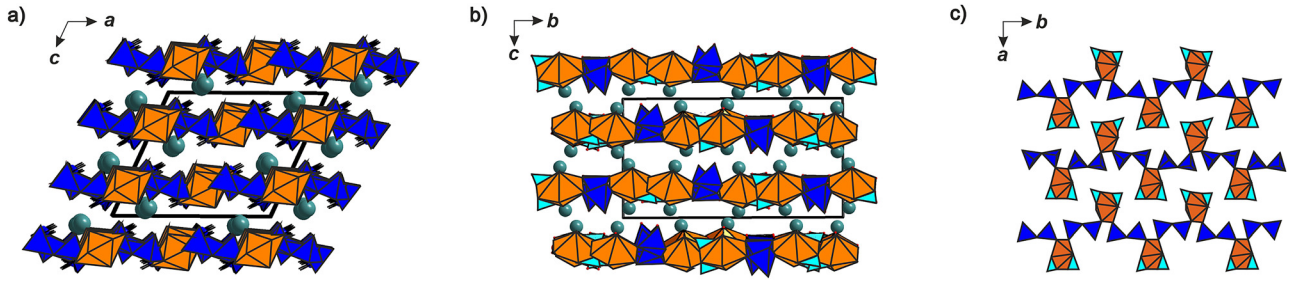

Figure 4: General projection of the structure of $Rb_2[(UO_2)(Cr_2O_7)(NO_3)_2]$ along the *b* axis (a) and along the *a* axis (b). The chains alignment into pseudo-layers (c). The color scheme as in Figure 3.

uranyl and dichromate species, these graphs have very much in common (Figure 7). The graph of the $[(UO_2)(Cr_2O_7)(NO_3)_2]_2^{4-}$ dimer corresponds to a cycle containing four white and two black nodes (Figure 7a, b). Their fusion in a spirane-like mode results in the graph of the $[(UO_2)(Cr_2O_7)_2(H_2O)]^{2-}$ chain (Figure 7c, d), found in the structures of $(EMIM)_2(UO_2)(Cr_2O_7)_2(H_2O)$ [44] (EMIM = 1-ethyl-3-methylimidazolium) and $(H_2diaza\text{-}18\text{-}crown\text{-}6)_2[(UO_2)_2(Cr_2O_7)_4(H_2O)_2](H_2O)_3$ [52]. The graph for the chains in **1** (Figure 7e, f) can be produced by dissecting the previous one along the propagation line. In fact, the $[UO_2(Cr_2O_7)(NO_3)_2]^{2-}$ chain can be considered as a product of ring-opening polymerization of the $[UO_2(Cr_2O_7)(NO_3)_2]_2^{4-}$ dimer.

The compound **2** is isostructural to the γ-$(NH_4)_2Cr_3O_{10}$ (Table 2). Both compounds adopt the same space group and their unit-cell parameters differ by less than 0.05 Å which suggests complete solid solubility. The compound **3** is isostructural to δ-$K_2Cr_3O_{10}$.

In 1974, Lofgren et al. described three types or conformations of trichromate anion as distorted fragments of polymeric chains in the structure of CrO_3 [68]. Casari et al. [53] added three more conformations observed in the structures of $K_2Cr_3O_{10}$ [61], $(bpyzH)_2Cr_3O_{10}$ [62] (bpyz = bispyrazinium), and $(C_{20}H_{20}N_6)Cr_3O_{10}$ [69], and classified them based on the values of Cr–Cr–Cr angles which he considered as a descriptive index fort he configuration for

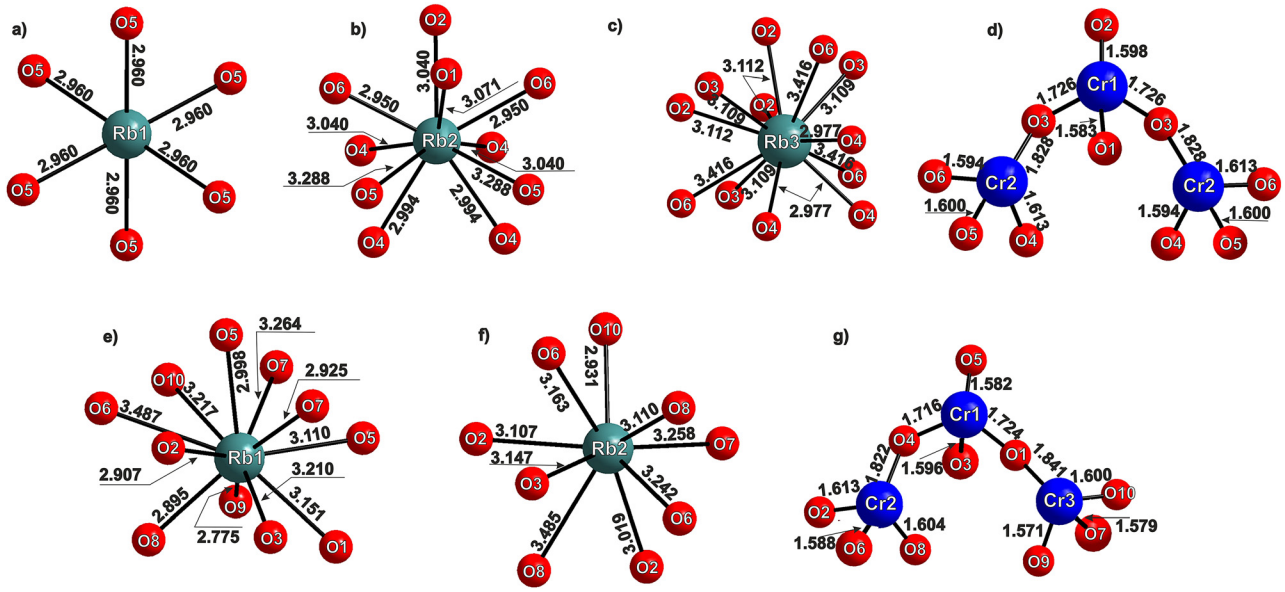

Figure 5: Coordination of Rb1 (a), Rb2 (b), Rb3 (c), and Cr (d) in the structure of **2** (γ-$Rb_2Cr_3O_{10}$). Coordination of Rb1 (e), Rb2 (f), and Cr (g) in the structure of **3** (δ-$Rb_2Cr_3O_{10}$).

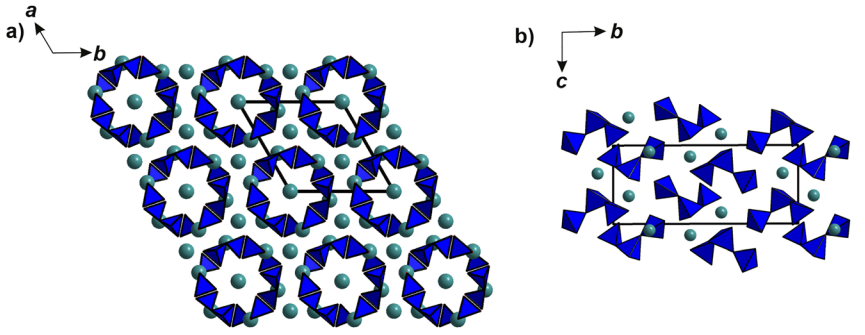

Figure 6: General projection of the structure of **2** along the *c* axis (a). General projection of the structure of **3** along the *a* axis (b).

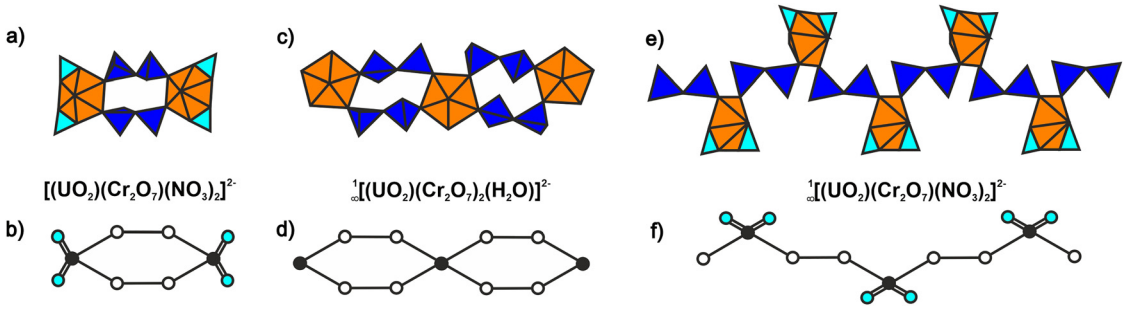

Figure 7: The 0D $[(UO_2)(Cr_2O_7)(NO_3)_2]_2^{4-}$ complex in the structure of $Cs_2(UO_2)(Cr_2O_7)(NO_3)_2$ (a) and its graph (b). The $[(UO_2)(Cr_2O_7)_2(H_2O)]^{2-}$ chain in the structure of $(EMIM)_2(UO_2)(Cr_2O_7)_2(H_2O)$ (c) and its graph (d). The $[(UO_2)(Cr_2O_7)(NO_3)_2]^{2-}$ chain in the structure of **1** (e) and its graph (f). The color scheme for (a), (c), and (e) as in Figure 3. For (b), (d), and (f) white nodes are Cr, black nodes are U and blue nodes are N.

the polychromate chains. The Cr–Cr–Cr angle in δ-$Rb_2Cr_3O_{10}$ is 90.62° while 90.25° in γ-$Rb_2Cr_3O_{10}$. The value in the hexagonal polymorph is very close to that in γ-$(NH_4)_2Cr_3O_{10}$ (90.04°). For the monoclinic forms ($P2_1/n$), this angle varies from 120.7 to 86.85° while in δ-$Rb_2Cr_3O_{10}$ it is close to those in hexagonal forms. This clearly indicates that these values are determined mostly by the nature of the cation but not of the polymorph. It is informative in the case of large organic cations which donate hydrogen bonds to the trichromate anions in directions determined

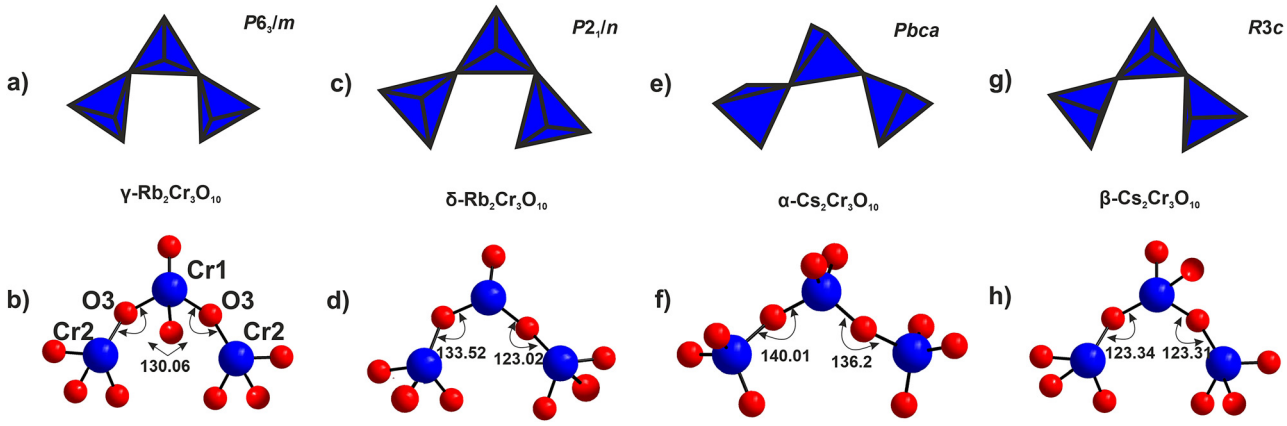

Figure 8: Topology and conformation of $Cr_3O_{10}^{2-}$ anion in the structures of γ-$Rb_2Cr_3O_{10}$ (a, b), δ-$Rb_2Cr_3O_{10}$ (c, d), α-$Cs_2Cr_3O_{10}$ (e, f), and β-$Cs_2Cr_3O_{10}$ (g, h) in polyhedral and ball-and-stick representation. Bond angles at the bridging oxygens are also shown.

by the positions of protonated nitrogen atoms. In these cases, the trichromate chains are forced to adjust their conformations to the shape of organic species and directions of hydrogen bonds. However, in the case of large alkali cations with relatively non-rigid coordination environments, the shape of the trichromate anions, hence the Cr–Cr–Cr angle, is less variable.

Four conformations can be formally distinguished in the structures of alkali and ammonium trichromates (Figure 8). The highest-symmetrical one (Figure 8a, b) exists in the structures of **2** and γ-$(NH_4)_2Cr_3O_{10}$. Both Cr–O–Cr angles equal 130.05°. Larger dissimilarities in rotation angles are observed in the monoclinic (Figure 8c, d) and orthorhombic (Figure 8e, f) polymorphs (133.52 and 123.04° for the former and 140.01 and 136.01° for the latter). Only β-$Cs_2Cr_3O_{10}$ [61] represents the trigonal (*R3c*) polymorph wherein these angles equal 123.34 and 123.31°.

Unfortunately, trichromates of univalent cations have not been studied systematically. According to Table 2, the most commonly represented is the orthorhombic (α) form observed among compounds of Rb, Cs, and NH_4, *i.e.*, the largest alkali species. Prior to this work, other polymorphic forms had but one representative, the δ form being unique for the compound of potassium, the smaller contributor to the trichromate family. Note that despite widespread use of Na_2CrO_4 and $Na_2Cr_2O_7$ as Cr^{VI} sources, sodium trichromate is unknown to date, which suggests that Na^+ and particularly Li^+ are too small to combine with the large $Cr_3O_{10}^{2-}$ anions. No trichromate has also been reported for Tl and Ag which form low-soluble dichromates. The β polymorph remains unique and likely to be stabilized by the largest Cs^+ cation. The γ polymorph is hitherto observed among compounds of rubidium and ammonium. Our data indicate that γ-$Rb_2Cr_3O_{10}$ crystallizes at higher pH values compared to δ-$Rb_2Cr_3O_{10}$. It is thus possible that transformation of hexagonal form to monoclinic occurs upon increasing acidity of the solution. The common appearance of the orthorhombic structure can be explained by the fact that syntheses are usually carried out at pH ≥ 3. Additional factors, including overall concentration of Cr^{VI} and presence of uranium species, as well as small temperature variations, might also have contributed to formation of the two polymorphs of $Rb_2Cr_3O_{10}$. Systematic studies necessary for estimating their possible roles are of interest lie outside the scope of the current paper.

5 Concluding remarks

Our studies of rubidium – uranyl chromates resulted in three novel compounds, $Rb_2[(UO_2)(Cr_2O_7)(NO_3)_2]$, γ-$Rb_2Cr_3O_{10}$, and δ-$Rb_2Cr_3O_{10}$ which were structurally characterized. They were produced upon evaporation of thermally pre-treated solution. The crystals are formed in acidic media in the sequence **1** (pH = 2.5), **2** (pH = 2), and **3** (pH = 1.5). Note that crystallization of all known uranyl dichromates occurs at similar conditions. Addition of CrO_3 to the solutions of uranyl salts increases their acidity, therefore they contain relatively low amounts of CrO_4^{2-} compared to polycromates, $Cr_2O_7^{2-}$ in particular [70]. It is the latter that contribute to the formation of architectures shown in Figure 1. It is possible that their hydrolysis accelerates at elevated temperatures producing more CrO_4^{2-} or $HCrO_4^-$ monomeric anions. A similar conclusion can be made when comparing the structures of the initial reagents. The structure of CrO_3 is comprised of pyroxene-like chains of vertex-sharing CrO_4 tetrahedra [68]. In alkali monochromates (K_2CrO_4, Na_2CrO_4) the isolated CrO_4^{2-} are linked together by the alkali cations. The dissolution of CrO_3 in initially neutral media adds the polychromate

anions while dissolution of alkali chromates produces mostly monomeric chromate anions.

The edges of NO_3^- triangles and equatorial planes of UrO_5 (UrO_6) bipyramids quite coincide in size which enhances κ^2-coordination of nitrate to the uranyl cation, akin to carbonate and carboxylate anions. In acidic media, *i.e.*, under chromate-poor conditions, one can expect formation of species with relatively low CrO_4^{2-}:UO_2^{2+} ratio (*e.g.*, 1:1). Evaporation of such solutions leads to formation of polychromate anions [56]. The vacant coordination sites in the UrO_n polyhedra can be occupied, dependent by the concentration ratio, by either terminal nitrate groups or by bridging dichromate groups. When alkali chromates are used as the Cr^{VI} source, the monomeric CrO_4^{2-} anions are essentially enough abundant to produce complexes with higher CrO_4^{2-}:UO_2^{2+} ratios which may be also favored from electrostatic viewpoint.

Acknowledgments: Technical support by the SPbSU X-ray Diffraction and Microscopy and Microanalysis Resource Centers is gratefully acknowledged.

Author contributions: All the authors have accepted responsibility for the entire content of this submitted manuscript and approved submission.

Research funding: This work was financially supported by the Russian Science Foundation through the grant 16-17-10085.

Conflict of interest statement: The authors declare no conflicts of interest regarding this article.

References

1. Hazen R. M., Ewing R. C., Sverjensky D. A. Evolution of uranium and thorium minerals. *Am. Mineral.* 2009, *94*, 1293–1311.
2. Halasyamani P. S., Francis R. J., Bee J. S., O'Hare D. Variable dimensionality in the uranium fluoride/2-methyl-piperazine system: syntheses and structures of UFO-5, 6, and 7; zero, one, and two dimensional materials with unprecedented topologies. *Mater Res. Soc. Symp.* 1999, *547*, 383–388.
3. Romanchuk A. Y., Vlasova I. E., Kalmykov S. N. Speciation of uranium and plutonium from nuclear legacy sites to the environment: a mini review. *Front. Chem.* 2020, *8*, 1–10.
4. Romanchuk A. Y., Kalmykov S. N. *Function of Colloidal and Nanoparticles in the Sorption of Radionuclides (Book Chapter). Behavior of Radionuclides in the Environment I: Function of Particles in Aquatic System*; Springer: Singapore, 2020; pp. 151–176.
5. Lebedev V. A., Piscounov V. M. Analysis of the vat residue of radioactive waste and the development of matrix mixtures for immobilization of the compound on the basis of mineral binders nanomodified. *J. Min. Inst.* 2013, *1*, 55–58.
6. Siidra O. I., Nazarchuk E. V., Charkin D. O., Ikhalaynen Y. A., Sharikov M. I. Open-framework sodium uranyl selenate and sodium uranyl sulfate with protonated morpholino-N-acetic acid. *Z. Kristallogr. - Cryst. Mater.* 2019, *234*, 109–118.
7. Siidra O. I., Nazarchuk E. V., Charkin D. O., Bocharov S. N., Sharikov M. I. Uranyl sulfate nanotubules templated by N-phenylglycine. *Nanomaterials* 2018, *8*, 216–220.
8. Krivovichev S. V., Burns P. C., Tananaev I. G., Eds. *Structural Chemistry of Inorganic Actinide Compounds*; Elsevier: Amsterdam, 2007; p. 494.
9. Doran M. B., Norquist A. J., O'Hare D. Exploration of composition space in templated uranium sulfates. *Inorg. Chem.* 2003, *42*, 6989–6995.
10. Nazarchuk E. V., Ikhalaynen Y. A., Charkin D. O., Siidra O. I., Kalmykov S. N., Borisov A. S. Effect of solution acidity on the structure of amino acid-bearing uranyl compounds. *Radiochim. Acta* 2019, *107*, 311–325.
11. Nazarchuk E. V., Siidra O. I., Charkin D. O. Specific features of the crystal chemistry of layered uranyl compounds with the ratio UO_2:TO_4 = 5:8 ($T = S^{6+}$, Cr^{6+}, Se^{6+}, Mo^{6+}). *Radiochemistry* 2018, *60*, 352–361.
12. Krivovichev S. V. Structural crystallography of inorganic oxysalts. *Crystallogr. Rev.* 2009, *15*, 279–281.
13. Nazarchuk E. V., Charkin D. O., Siidra O. I., Kalmykov S. N. Organically templated layered uranyl molybdate $[C_3H_9NH^+]_4[(UO_2)_3(MoO_4)_5]$ structurally based on mineral-related modular units. *Minerals* 2020, *10*, 659–665.
14. Nazarchuk E. V., Siidra O. I., Krivovichev S. V. Synthesis and crystal structure of $Ag_2[(UO_2)_6(MoO_4)_7(H_2O)_2](H_2O)_2$. *Radiochemistry* 2016, *58*, 1–50.
15. Nazarchuk E. V., Siidra O. I., Krivovichev S. V., Malcherek T., Depmeier W. First mixed alkaline uranyl molybdates: synthesis and crystal structures of $CsNa_3[(UO_2)_4O_4(Mo_2O_8)]$ and $Cs_2Na_8[(UO_2)_8O_8(Mo_5O_{20})]$. *Z. Anorg. Allg. Chem.* 2009, *635*, 1231–1235.
16. Nazarchuk E. V., Krivovichev S. V., Burns P. C. Crystal structure of $Tl_2[(UO_2)_2(MoO_4)3]$ and crystal chemistry of the compounds $M_2[(UO_2)_2(MoO_4)_3]$ (M = Tl, Rb, Cs). *Radiochemistry* 2005, *47*, 447–451.
17. Krivovichev S. V., Burns P. C., Armbruster T., Nazarchuk E. V., Depmeier W. Chiral open-framework uranyl molybdates. 2. Flexibility of the U:Mo = 6:7 frameworks: syntheses and crystal structures of $(UO_2)_{0.82}[C_8H_{20}N]_{0.36}[(UO_2)_6(MoO_4)_7(H_2O)_2](H_2O)n$ and $[C_6H_{14}N_2][(UO_2)_6(MoO_4)_7(H_2O)_2](H_2O)_m$. *Microporous Mesoporous Mater.* 2005, *78*, 217–224.
18. Krivovichev S. V., Armbruster T., Chernyshov D. Y., Nazarchuk E. V., Depmeier W. Chiral open-framework uranyl molybdates. 3. Synthesis, structure and the $C222_1 \rightarrow P2_12_12_1$ low-temperature phase transition of $[C_6H_{16}N]_2[(UO_2)_6(MoO_4)_7(H_2O)_2](H_2O)_2$. *Microporous Mesoporous Mater.* 2005, *78*, 225–234.
19. Krivovichev S. V., Cahill C. L., Nazarchuk E. V., Armbruster T., Depmeier W. Chiral open-framework uranyl molybdates. 1. Topological diversity: synthesis and crystal structure of $[(C_2H_5)_2NH_2]_2[(UO_2)_4(MoO_4)_5(H_2O)](H_2O)$. *Microporous Mesoporous Mater.* 2005, *78*, 209–215.
20. Nazarchuk E. V., Krivovichev S. V., Filatov S. K. Phase transitions and high-temperature crystal chemistry of polymorphous modifications of $Cs_2(UO_2)_2(MoO_4)$. *Radiochemistry* 2004, *46*, 438–440.
21. Obbade S., Dion C., Bekaert E., Yagoubi S., Saadi M., Abraham F. Synthesis and crystal structure of new uranyl tungstates $M_2(UO_2)(W_2O_8)$ (M = Na, K), $M_2(UO_2)_2(WO_5)O$ (M = K, Rb) and $Na_{10}(UO_2)_8(W_5O_{20})O_8$. *J. Solid State Chem.* 2003, *172*, 305–318.

22. Alekseev E. V., Krivovichev S. V., Depmeier W., Armbruster T., Katzke H., Suleimanov E. V., Chuprunov E. V. One-dimensional chains in uranyl tungstates: syntheses and structures of $A_8[(UO_2)_4(WO_4)_4(WO_5)_2]$ (A = Rb,Cs) and $Rb_6[(UO_2)_2O(WO_4)_4]$. *J. Solid State Chem.* 2006, *179*, 2977–2987.
23. Alekseev E. V., Krivovichev S. V., Depmeier W., Malcherek T., Suleimanov E. V., Chuprunov E. V. The crystal structure of $Li_4[(UO_2)_2(W_2O_{10})]$ and crystal chemistry of Li uranyl tungstates. *Z. Kristallogr. - Cryst. Mater.* 2007, *222*, 391–395.
24. Siidra O. I., Nazarchuk E. V., Petrunin A. A., Kayukov R. A., Krivovichev S. V. Nanoscale hemispheres in novel mixed-valent uranyl chromate(V,VI), $(C_3NH_{10})_{10}[(UO_2)_{13}(Cr_{12}O_{42})(CrO_4)_6(H_2O)_6](H_2O)6$. *Inorg. Chem.* 2012, *51*, 9162–9164.
25. Siidra O., Nazarchuk E., Bocharov S., Depmeier W., Zadoya A. Formation of co-racemic uranyl chromate constructed from chiral layers of different topology. *Acta Crystallogr.* 2017, *B73*, 101–111.
26. Nazarchuk E. V., Siidra O. I., Kayukov R. A. Synthesis and crystal-chemical features of two new uranyl chromates with the structures derived from $[(UO_2)(TO_4)(H_2O)_n]^0$ (T = Cr^{6+}, S^{6+}, Se^{6+}, n = 0–2). *Radiochemistry* 2016, *58*, 571–577.
27. Nazarchuk E. V., Siidra O. I., Zadoya A. I., Agakhanov A. A. Host-guest structural architectures in hydrous alkaline (Li, K) uranyl chromates and dichromates. *Inorg. Chem. Commun.* 2015, *62*, 15–18.
28. Siidra O. I., Nazarchuk E. V., Krivovichev S. V. Mixed-ligand coordination of the $(UO_2)^{2+}$ cation and apophyllite topology of uranyl chlorochromate layer in the structure of $((CH_3)_2CHNH_3)[(UO_2)(CrO_4)Cl(H_2O)]$. *Z. Kristallogr. - Cryst. Mater.* 2012, *227*, 530–534.
29. Siidra O. I., Nazarchuk E. V., Krivovichev S. V. Isopropylammonium layered uranyl chromates: syntheses and crystal structures of $[(CH_3)_2CHNH_3]_3[(UO_2)_3(CrO_4)_2O(OH)_3]$ and $[(CH_3)_2CHNH_3]_2[(UO_2)_2(CrO_4)_3(H_2O)]$. *Z. Anorg. Allg. Chem.* 2012, *638*, 976–981.
30. Siidra O. I., Nazarchuk E. V., Krivovichev S. V. Highly kinked uranyl chromate nitrate layers in the crystal structures of $A[(UO_2)(CrO_4)(NO_3)]$ (A = K, Rb). *Z. Anorg. Allg. Chem.* 2012, *638*, 982–986.
31. Siidra O. I., Nazarchuk E. V., Krivovichev S. V. Syntheses and crystal structures of two novel alkaline uranyl chromates $A_2(UO_2)(CrO_4)_2$ (A = Rb, Cs) with bidentate coordination mode of uranyl ions by chromate anions. *J. Solid State Chem.* 2012, *187*, 286–29.
32. Siidra O. I., Nazarchuk E. V., Krivovichev S. V. Unprecedented bidentate coordination of the uranyl cation by the chromate anion in the structure of $[(CH_3)_2CHNH_3]_2[UO_2(CrO_4)_2]$. *Eur. J. Inorg. Chem.* 2012, *2*, 194–197.
33. Herbst R. S., Law J. D., Todd T. A., Romanovskiy V. N., Smirnov I. V., Babain V. A., Esimantovskiy V. N., Zaitsev B. N. Development of the universal extraction (unex) process for the simultaneous recovery of Cs, Sr, and actinides from acidic radioactive wastes. *Separ. Sci. Technol.* 2003, *38*, 2685.
34. Delmore J. E., Snyder D. C., Tranter T., Mann N. Cesium isotope ratios as indicators of nuclear power plant operations. *J. Environ. Radioact.* 2011, *102*, 1008–11.
35. Degueldre C. A., Dawson R. J., Najdanovic-Visak V. Nuclear fuel cycle, with a liquid ore and fuel: toward renewable energy. *Sustain. Energy Fuels* 2019, *3*, 1693–1700.
36. Gabaraev B. A., Smirnov Yu., Cherepnin Yu. S. *Nuclear Power Engineering of the XXI Century*; MEI Publishing House: Moscow, 2013.
37. Babichev B. A., Esimantovskiy V. M., Kavetsky A. G., Fireplaces V. M. Characteristics of the fraction containing curium and rare earth elements obtained during processing of VVER-1000 SNF. *Proc. Khlopin Inst.* 2003, *10*, 106–117.
38. Kovba L. M., Ippolitova E. A., Simanov Y. P., Spitsyn V. I. The crystal structure of uranates. 1. Uranates with tetragonal layers $(UO_2)O_2$. *Dokl. RAN* 1958, *120*, 1042–1044.
39. Zachariasen W. H. Crystal chemical studies of the 5f-Series of elements. XX. The crystal structure of tri-potassium uranyl fluoride. *Acta Crystallogr.* 1954, *7*, 783–787.
40. Sundberg I., Sillén L. G. On the crystal structure of KUO_2VO_4 (Synthetic anhydrous carnotite). *Ark. Kem. Mineral. Geol.* 1949, *1*, 337–351.
41. Serezhkina L. B., Trunov V. K., Kholodkovskaya L. N., Kuchumova N. V. Crystal structure of $KUO_2CrO_4(OH)$ $1.5(H_2O)$. *Coord. Chem.* 1990, *16*, 1288–1291.
42. Sykora R. E., McDaniel S. M., Wells D. M., Albrecht Schmitt T. E. Mixed-metal uranium(VI) iodates: hydrothermal syntheses, structures and reactivity of $Rb(UO_2(CrO_4)(IO_3)(H_2O))$, $A_2(UO_2(CrO_4)(IO_3)_2)$ (A = K, Rb, Cs) and $K_2(UO_2(MoO_4)(IO_3)_2)$. *Inorg. Chem.* 2002, *41*, 5126–5132.
43. Verevkin A. G., Vologzhanina A. V., Serezhkina L. B., Serezhkin V. N. X-ray diffraction study of $Rb_2[(UO_2)_2(CrO_4)_3(H_2O)_2]$ $4H_2O$. *Kristallografiya* 2010, *55*, 645–650.
44. Siidra O. I., Nazarchuk E. V., Suknotova A. N., Kayukov R. A., Krivovichev S. V. Cr(VI) trioxide as a starting material for the synthesis of novel zero-, one-, and two-dimensional uranyl dichromates and chromate-dichromates. *Inorg. Chem.* 2013, *52*, 4729–4735.
45. Siidra O. I., Nazarchuk E. V., Bocharov S. N., Depmeier W., Kayukov R. A. Microporous uranyl chromates successively formed by evaporation from acidic solution. *Z. Kristallogr. - Cryst. Mater.* 2018, *233*, 1–8.
46. Murphy G. L., Langer E. M., Walter O. B., Wang Y. C., Wang S. C., Alekseev E. V. Insights into the structural chemistry of anhydrous and hydrous hexavalent uranium and neptunium dinitrato, trinitrato, and tetranitrato complexes. *Inorg. Chem.* 2020, *59*, 7204–7215.
47. Doran M. B., Norquist A. J., Hare D. O. catena-Poly [tetramethylammonium [[(nitrato-κ^2-O,O)dioxouranium]-mue3-sulfato]]. *Acta Crystallogr.* 2003, *E59*, m373–m375.
48. Liu D. S., Huang G. S., Luo Q. Y., Xu Y. P., Li X. F. Poly [tetramethylammonium [nitratouranyl-μ^3-selenito]]. *Acta Crystallogr.* 2006, *E62*, m1584–m1585.
49. Siidra O. I., Nazarchuk E. V., Zadoya A. I. Novel $[(UO_2)O_6(NO_3)_n]$ (n = 1, 2) based units in organically templated uranyl compounds. *Inorg. Chem. Commun.* 2014, *50*, 4–7.
50. Nazarchuk E. V., Charkin D. O., Siidra O. I., Gurzhiy V. V. Crystal-chemical features of U(VI) compounds with inorganic complexes derived from $[(UO_2)(TO_4)(H_2O)_n]$, T = S, Cr, Se: synthesis and crystal structures of two new uranyl sulfates. *Radiochemistry* 2018, *60*, 345–351.
51. Krivovichev S. V., Burns P. C. Structural topology of potassium uranyl chromates: crystal structures of $K_8[(UO_2)(CrO_4)_4](NO_3)_2$, $K_5[(UO_2)(CrO_4)_3](NO_3)(H_2O)_3$, $K_4[(UO_2)_3(CrO_4)_5](H_2O)_8$ and $K_2[(UO_2)_2(CrO_4)_3(H_2O)_2](H_2O)_4$. *Z. Kristallogr.* 2003, *218*, 725–732.
52. Siidra O. I., Nazarchuk E. V., Charkin D. O., Kalmykov S. N., Zadoya A. I. Complex uranyl dichromates templated by aza-crowns. *Crystals* 2018, *8*, 462–474.

53. Casari B. M., Oberg E., Langer V. The orthorhombic polymorph of diammonium trichromate(VI) decaoxide, α–$(NH_4)_2Cr_3O_{10}$. *J. Chem. Crystallogr.* 2007, *37*, 135–140.
54. Gili P., Lorenzo-Louis P. A. Compounds of chromium(VI) as ligands. *Coord. Chem. Rev.* 1999, *193-195*, 747–768.
55. Nazarchuk E. V., Charkin D. O., Kozlov D. V., Siidra O. I., Kalmykov S. N. Topological analysis of the layered uranyl compounds bearing slabs with UO_2:TO_4 ratio of 2:3. *Radiochim. Acta* 2019, *108*, 249–260.
56. Siidra O. I., Nazarchuk E. V., Sysoeva E. V., Kayukov R. A., Depmeier W. Isolated uranyl chromate and polychromate units in crown ether templated compounds. *Eur. J. Inorg. Chem.* 2014, *2014*, 5495–5498.
57. Kolitsch U. Alpha-$(Cs_2Cr_3O_{10})$. *Acta Crystallogr.* 2003, *E59*, i164–i166.
58. Loefgren P. The crystal structure of $Rb_2Cr_3O_{10}$. *Chem. Scripta* 1974, *5*, 91–96.
59. Mattes R., Meschede W. Zur struktur des $Cr_3O_{10}^{(2-)}$ – ions in beta-$Cs_2Cr_3O_{10}$. *Z. Anorg. Allg. Chem.* 1973, *395*, 216–222.
60. Blum D., Guitel J. C. Structure de la forme hexagonale du trichromate d'ammonium: $(NH_4)_2$. *Acta Crystallogr.* 1980, *B36*, 135–137.
61. Blum D., Averbuch-Pouchot M. T., Guitel J. C. Structure du tripolychromate de potassium $K_2Cr_3O_{10}$. *Acta Crystallogr.* 1979, *B35*, 454–456.
62. Sheldrick G. M. Short history of SHELX. *Acta Crystallogr.* 2008, *A64*, 112–122.
63. Pressprich M. R., Willet R. D., Poshusta R. D., Saunders S. C., Davis H. B., Gard G. L. Preparation and crystal structure of dipyrazinium trichromate and bond length correlation for chromate anions of the form Cr_nO_{2-3n+1}. *Inorg. Chem.* 1988, *27*, 260.
64. Betke U., Wickleder M. Oleum and sulfuric acid as reaction media: the actinide examples $UO_2(S_2O_7)$ – lt (low temperature), $UO_2(S_2O_7)$ – ht (high temperature), $UO_2(HSO_4)_2$, $An(SO_4)_2$ (An = Th, U), $Th_4(HSO_4)_2(SO_4)_7$ and $Th(HSO_4)_2(SO_4)$. *Eur. J. Inorg. Chem.* 2012, *2*, 306–317.
65. Yu N., Kegler P., Klepov V. V., Dellen J. Influence of extreme conditions on the formation and structures of caesium uranium(VI) arsenates. *Dalton Trans.* 2015, *44*, 20735–20744.
66. Alekseev E. S., Krivovichev S. V., Depmeier W. $K_2[(UO_2)As_2O_7]$ – the first uranium polyarsenate. *Z. Anorg. Allg. Chem.* 2007, *633*, 1125–1126.
67. Linde S. A., Gorbunova Yu. E., Lavrov A. V., Pobedina A. B. Synthesis and structure of crystals of uranyl pyrophosphates $M_2UO_2P_2O_7$ (*M* = rubidium, cesium). *Neorg. Mater.* 1981, *17*, 1062–1066.
68. Stephens J. S., Cruickshank D. W. J. The crystal structure of (CrO_3) infinite. *Acta Crystallogr.* 1970, *B26*, 222–226.
69. Garrison J. C., Simons R. S., Talley J. M., Wesdemiotis C., Tessier C. A., Youngs W. J. Synthesis and structural characterization of an imidazolium-linked cyclophane and the silver complex of an N-heterocyclic carbene-linked cyclophane. *Organometallics* 2001, *20*, 1276.
70. Cui W., Li P., Zheng S., Zhang H., Liu C., Chen Y., Zhang Y. Phase equilibria for the $KHSO_4$–H_2SO_4–H_2O and $KHSO_4$–CrO_3–H_2SO_4–H_2O systems at 313.15 K. *J. Chem. Eng. Data* 2016, *61*, 354–358.

Supplementary Material: The online version of this article offers supplementary material (https://doi.org/10.1515/zkri-2020-0078).